Optik 127 (2016) 2193–2196

Contents lists available at ScienceDirect

Optik

journal homepage: www.elsevier.de/ijleo

Study of reflection-typed LED surgical shadowless lamp with thin film Ag-based metallic glass

C.T. Pan [a,*], Y.C. Chen [a], T.L. Yang [a], Po-Hsun Lin [a], Po-Hung Lin [a], J.C. Huang [b]

[a] Department of Mechanical and Electro-Mechanical Engineering, Center for Nanoscience and Nanotechnology, National Sun Yat-Sen University, Kaohsiung 80424, Taiwan

[b] Department of Materials and Optoelectronic Science, Center for Nanoscience and Nanotechnology, National Sun Yat-Sen University, Kaohsiung 80424, Taiwan

ARTICLE INFO

Article history:
Received 31 May 2015
Accepted 22 November 2015

Keywords:
Surgical shadowless lamp
Elliptical curve
Thin film metallic glass
Light-emitting diodes

ABSTRACT

Traditional surgical shadowless halogen lamp can cause mercury pollution and increase heat radiation. In this study, single one light-emitting diode (LED) is used as light source for shadowless surgical light, whose light performance is comparable with traditional halogen light bulbs. This surgical shadowless lamp with multi-focal ellipsoidal curve reflector was designed and made. Reflection-typed shadowless surgical light is better than projection-typed one. This design can reduce significantly the use of LEDs. Various recipes of Ag–Cu–Al thin film metallic glass (Ag-based TFMG) were determined and coated on the curve as reflector materials, possessing great mechanical strength and anti-bacterial effect. The Ag-based can affect the light temperature and light color. Appropriate alloy elements of this metallic glass could be formulated to absorb IR range wavelength to reduce the wound damage during surgery. For the optical measurement, the central illuminance (Ec) was 110,500 lx, d_{50}/d_{10} was 58.9% and working depth was 32.8 cm. The shadow dilution with single mask and double masks were 58.96% and 56.16%, respectively. Then, for the combination of tubes, the shadow dilution of lamp with single mask and double masks were 57.46% and 58.03%, respectively. The experimental results meet the rule of IEC-60601-2-41.

1. Introduction

Currently, several important characteristics are required for surgical lighting, for example, light quantity, shadow reduction, light beam directionality, heat production, and light color. The challenge of surgical lighting has further been increased since the recent introduction of the LED to operating room (OR) light was an emerging lighting technology [1]. In OR, lamps heat may cause discomfort to the surgeon and patients while operating [2]. Heat problems such as dehydration and burn wounds have been reported for the traditional lighting filter without the infrared (IR). However, the spectrum of LEDs contains mainly visible wavelengths [3]. Thus, LED luminaires can reduce heat problems due to the absence of IR radiation. The design of a surgical luminaire is a complex task because various optical requirements should be met such as thermal and mechanical requirements [4].

There are several methods of stacked elliptic curve reflectors to design and fabricate surgical lamps, such as refracting light to target plane by Fresnel lens which is composed of many different prisms [5], and utilizing continuous profiles to enhance the uniformity of light distribution [6]. Moreover, multi-reflector surgical lamp which combined parabola surface and elliptic curve as reflector and placed the light source at co-focus was brought up in 1990 by Harry [7]. In this study, a non-coaxial method was used to design a surgical shadowless lamp with multi-ellipsoidal curve layers. A recipe of Ag–Cu–Al TFMG (Ag-based thin film metallic glass) with high reflection was determined and used as reflective coating materials on the ellipsoidal curves. Ag-based TFMG are materials of amorphous metal alloy with high optical wavelength selectivity, low surface roughness, high anti-bacteria and good protective coating. Therefore its optical performance as the light reflective coating materials in OR are better than the crystalline metal alloy. Most importantly, the TFMG contains silver base that can reach the anti-bacterial requirements in the operating room. The deep wound of patient was modeled by a black tube; and the head of the surgeon and a surgical assistant were modeled by two masks that partially block the light beam [8]. The European Standard NEN-EN-IEC 60601-2-41 [3] describes various requirements for basic safety and necessary performance of surgical luminaires [9]. The light intensity, beam width and color rendering index (CRI) were characterized. In this study, all of the measured results meet with regulations [10,11].

* Corresponding author. Tel.: +886 75252000.
E-mail address: panct@mail.nsysu.edu.tw (C.T. Pan).

http://dx.doi.org/10.1016/j.ijleo.2015.11.150
0030-4026/

Table 1
Specifications of LED light source.

CCT (K)	CRI	Flux (lm)	Forward voltage (V)	Operating current I_F (A)	Viewing angle (degree)	Effective emitting area (mm^2)
5000	95	7390	37	0.9	120	12

2. Design methods

LED light source is a Lambertian distribution, and the light emission of half intensity angle is 60° that affects the d_{50}/d_{10} of light distribution on the target plane. A reflector which is stacked by multilayer elliptic curves with different focuses is designed to solve the problem. Besides, each elliptic curve is an independent light source that makes light emit to the target plane from different angles, and the goal of the shadowless can be achieved. Fig. 1 and Eq. (1) are applied to construct the non-coaxial focus of ellipsoidal curves. The ellipse equation is used to calculate the multi-ellipsoidal curves.

$$\sqrt{\left(x-x_{f1}\right)^2+\left(y-y_{f1}\right)^2}+\sqrt{\left(x-x_{f2}\right)^2+\left(y-y_{f2}\right)^2}=2a \qquad (1)$$

where x_{f1} and y_{f1} are the coordinates of f_1; x_{f2} and y_{f2} are the coordinates of f_2, and a is the half-length of major axis.

The diameter of the illuminated area on the target plane and the angle between emitted light I and vertical coordinate were described in Fig. 1. Then, the coordinates of points P_1 and T_1 can be obtained, and the $\overline{P_1T_1}$ equation can be calculated by point-slope formula (Eq. (2)).

$$Y-Y_T=m(X-X_T) \qquad (2)$$

where m is slope of $\overline{P_1T_1}$. X_T and Y_T are the coordinates of T_1 point and coordinate O (0,0) was set as light source.

For this design, the first focus of each ellipsoidal curve is set as O (0,0) and the other focus is set at different locations according to geometrical design. This purpose is to reduce the number of light rays blocked by masks before the light reaches the target plane. Therefore, the shadow dilution on the target plane can be reduced. Moreover, the shadow dilution was defined as the central illuminance without mask divided by that with mask.

According to the rule, the light spot diameter d_t on the target plane is set as 300 mm. The distance between light source and target plane is set as 1000 mm. Fig. 1(a) shows that the ray trace went through the gap between the double masks tangential to R_1 and reached to T_1. Thus, the intersection of L_1 and emitted light I was defined as P_1. Likewise, the coordinates of P_2 and f_2 can be obtained. Therefore, the E_1 equation can be calculated by f_1, f_2, P_1 using Eq. (1).

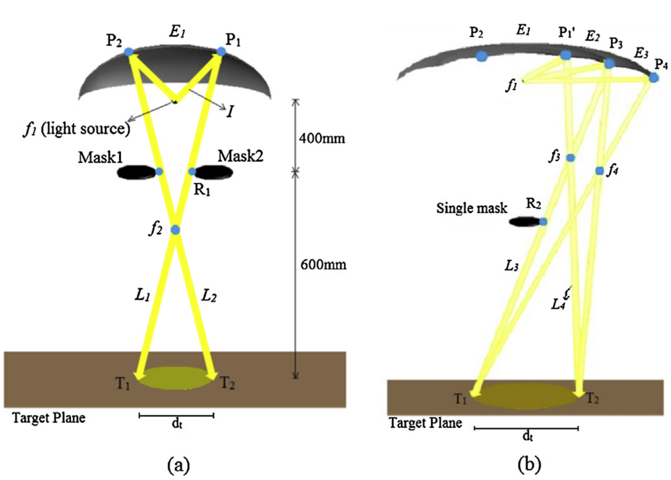

Fig. 1. Construction of non-coaxial focus of ellipsoidal curve (a) the geometry and location of the double mask and (b) single mask.

The purpose of E_1 was used to reflect light to target plane without being blocked by the double masks.

For the second and third ellipsoidal curves, Fig. 1(b) shows the purpose of E_2 and E_3 ellipsoidal curve layers, which were designed to emit light to target plane without being blocked by the single mask. The emitted light passing through edge point R_2 of the single mask reached T_1. Moreover, the ray trace was reflected from P_1' and reached T_2, which is defined as L_4. Therefore, the E_2 equation can be calculated by f_1, f_3, P_1' and Eq. (1). With the same process, the P_4 and E_3 equation can be obtained.

In this study, the light source of CREE CXA1816 LED was purchased as the surgical light source. The packaged size of LED chip is 17.85 × 17.85 × 1.6 (mm^3) and the diameter is 12 mm. Table 1 shows that LED flux is 7390 lumen and viewing angle is 120°. Ag-based TFMG is adopted as reflective materials coated on the reflector by using E-beam evaporator. In the simulation, FRED commercial software was used to design the curves. In this study, various recipes of Ag-based TFMG were formulated and tested. Currently, the relatively high reflectivity of Ag-based TFMG at wavelength of visible light is about 85%, shown as Fig. 2. The Ag-based TFMG possesses great mechanical properties and antibacterial effect. Then, the center illuminance, d_{50}/d_{10} and shadow dilution are analyzed.

3. Results and discussion

Simulation of shadowless dilution using software FRED. Fig. 3(a) shows the surgical shadowless prototype. According to the surgical light regulations, the shadow dilutions with both mask and tube should be measured. Fig. 3(b) shows the black tube used to simulate the patient deep wound.

Fig. 4 shows the comparison of central illuminance (Ec) between different numbers of ellipsoidal curve layers. It reveals that Ec increased with the curve numbers. However, the illuminance reached a constant when the curve number was larger than three. Therefore, in this study, three ellipsoidal curve layers were adopted.

The blue dash line in Fig. 5(a) shows the comparison of shadow dilution between different numbers of curve layers with single mask. The shadow dilution shows similar trend as shown in Fig. 4. The black dash line in Fig. 5(a) shows the comparison of shadow dilution between different numbers of curve layers with double masks. Number 2 curve layers shows the highest shadow dilution because the double masks can block the light reflected from third

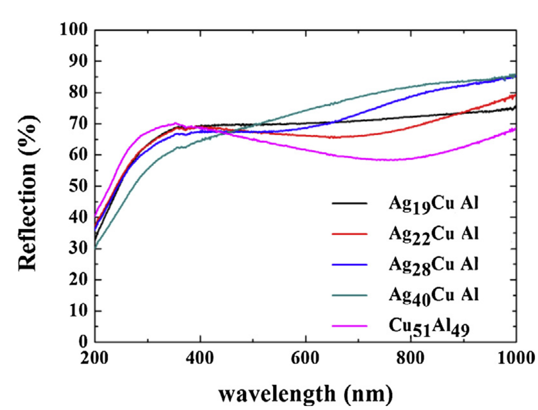

Fig. 2. Reflection of Ag-based (Ag19–Cu–Al) TFMG.

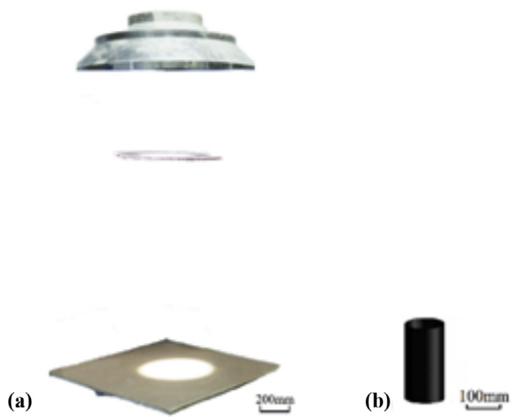

Fig. 3. Surgical shadowless system (a) measurement system (b) tube.

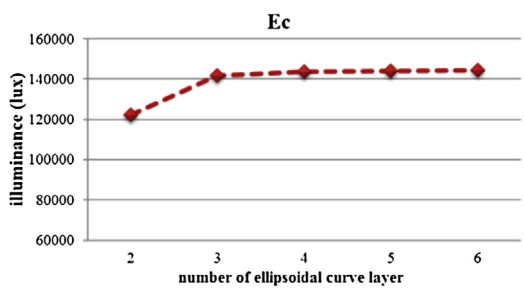

Fig. 4. Ec as a function of number curve layer.

curve layer. Thus, the shadow dilution decreased when the number of curve layer increased.

Fig. 5(b) shows the comparison of shadow dilution of single/double masks with tube. The shadow dilution decreased with the number of curve layers because the light reflected from high number of curve layers could be blocked by the sidewall of tube.

Fig. 6 shows that the d_{50}/d_{10} was higher than 60%, the uniformity of illuminance on target plane met with the regulation of the surgical light. For the simulation result of the shadow dilution, the shadow dilution with three curve layers was higher than average shadow dilution. The Ec of three curve layers was about 141,780 lx and the d_{50}/d_{10} was 60.8% and working depth was 36 cm. The shadow dilution with single mask and double masks were about 63.6% and 57.1%, respectively. For the consideration of tube, the shadow dilution with single mask and double masks were 59.6% and 61%, respectively. The result met with the regulation.

Apart from the Ec, shadowless dilution and the illuminance distribution on the target plane, the characteristics of light source can also affect the color fidelity. Thus, the characteristics of light reflected from Ag-based TFMG curve layer, as shown in Fig. 7, were measured. Ocean USB 2000+ spectrometer was used to measure the optical characteristics. Table 2 shows the color rendering index and color temperature of light reflected from Ag-based TFMG curve layers. The CRI changed from 92 to 85. Some light spectra could be

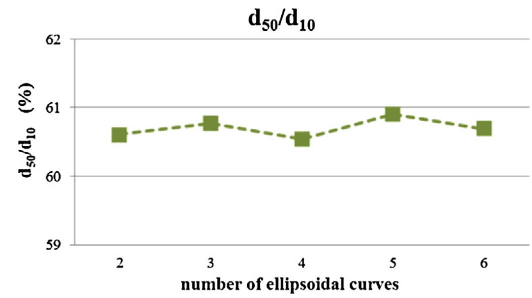

Fig. 6. Simulated d_{50}/d_{10} of surgical shadowless lamp with different numbers of curve layer.

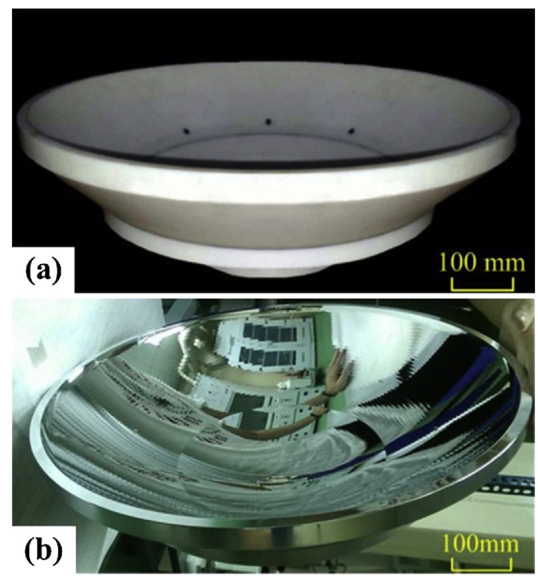

Fig. 7. Surgical shadowless reflector (a) without Ag-based TFMG (b) with Ag-based TFMG.

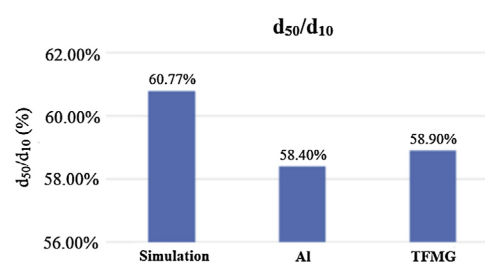

Fig. 8. Measured results of d_{50}/d_{10}.

absorbed by this film. This phenomena could create a new research field of how to adjust the CRI by using different TFMG recipes.

The Ec of light reflected from Ag-based TFMG film was 110,500 lx which was lower than simulated Ec 141,780 lx by 20%. Fig. 8 shows

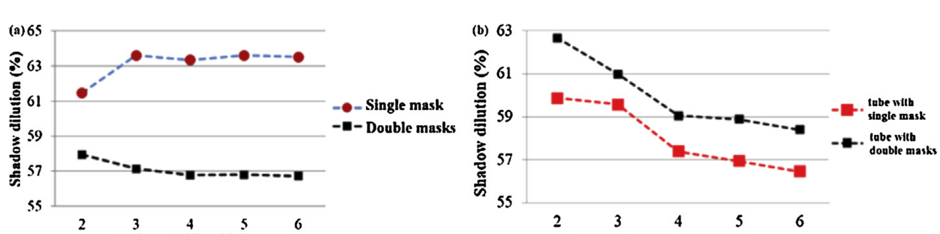

Fig. 5. (a) Comparison of shadow dilution of surgical shadowless lamp with single/double masks, (b) comparison of shadow dilution of single/double masks with tube.

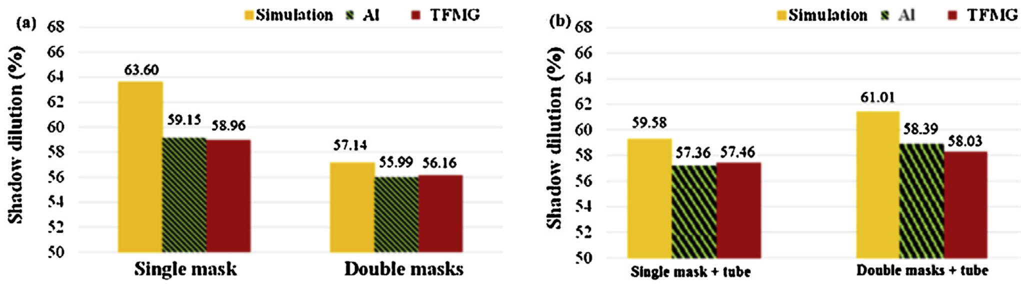

Fig. 9. Simulated and measured results of (a) shadow dilution, (b) shadow dilution with a tube.

Table 2
Spectrum measurements of LED and surgical shadowless reflector with Ag-based TFMG.

	CRI (Ra)	Color temperature CCT (K)
LED light source	92	5457
Ag-based TFMG film	85	4974

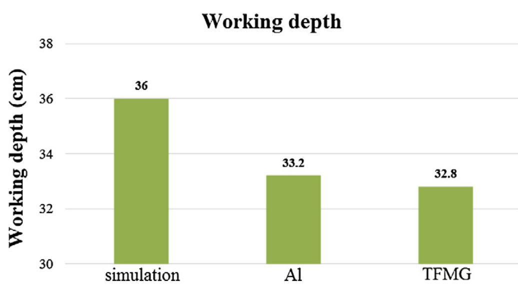

Fig. 10. Comparison of the measured and simulated working depth.

the comparison of d_{50}/d_{10} between simulation and measurement results. The measured d_{50}/d_{10} was 58.9%, lower than simulation of 60.77%. Fig. 9 shows the comparison of shadow dilution between the simulation and measurement results. The data show that all of the measured values were lower than simulated results. That could be due to the roughness of curve layer which could make part of light reflected out of target plane and reduce the d_{50}/d_{10}.

Fig. 10 shows comparison of the measured and simulated working depth. Since the maximum working depth is the height of the mask which blocked the area of d_{50}, a smaller d_{50} corresponds to a smaller working depth. Thus, the working depth was related with light trace which was influenced by curve layers. The data show that measured depth 32.8 cm was 10% lower than simulation of 36 cm.

4. Conclusions

In this study, the traditional projection-typed surgical shadowless lamp could be replaced with LED reflection-typed surgical shadowless lamp with multi-focal ellipsoidal curve layers to reduce the amount of light lamps and manufacturing cost. LED was used as light source and the various recipes of Ag–Cu–Al thin film metallic glass (Ag-based TFMG) were investigated and the optimal one was determined and used as coating materials of reflective curve layers. The Ag-based TFMG possesses excellent mechanical strength and anti-bacterial effect that is suitable for the OR environment. The simulated result shows three ellipsoidal curve layers was the optimal design. The Ec was 110,500 lx and d_{50}/d_{10} was 58.9% and working depth was 32.8 cm. The shadow dilution with single mask and double masks were 58.96% and 56.16%, respectively. Next, the mask was combined with a tube. The shadow dilution with single mask combined with tube, and double masks combined with tube were 57.46% and 58.03%, respectively.

References

[1] R. Marka, M. Vogl, C. Bartenbach, Multiple module lamp, U.S. Patent 7513645 B2, 2009.
[2] V.A. Jacobs, R. Van Gaever, B. Ribbens, W.R. Ryckaert, M. Diltoer, P. Rombauts, et al., Quality assessment of virtual prototypes of surgical luminaires using near-field ray-data, Leukos 9 (2013) 189–200.
[3] IEC, NEN-EN-IEC 60601-2-41:2010 Medical Electrical Equipment Part 2-41: Particular Requirements for Basic Safety and Essential Performance of Surgical Luminaires and Luminaires for Diagnosis, IEC, 2009.
[4] U. Matern, S. Koneczny, Safety, hazards and ergonomics in the operating room, Surg. Endosc. 21 (Nov) (2007) 1965–1969.
[5] H.H. Frazier, A.M. Smith, Surgical light with conical reflector. STERIS CORP (STER-Non-standard), U.S. Patent5913599A, 1999.
[6] U. Gampe, S. Greif, Reflector for a radiating luminous source and use of the 5same, U.S. Patent 6080464A1, 2000.
[7] W. Harry, Reflector for dental and surgical operating room lighting fixtures, U.S. Patent 4942507 A, 1990.
[8] Patkin, What surgeons want in operating rooms, Minim. Invasive Ther. Allied Technol. 12 (2003) 256–262.
[9] Y.F. Chuang, Profiles of shadowless reflector for operating lighting, U.S. Patent 6135602A, 2000.
[10] C.T. Pan, Y.C. Chen, T.L. Yang, P.H. Lin, P.H. Lin, C.C. Hsieh, Design of elliptic reflective LED surgical shadowless lamps using mathematical optical tracing algorithms, Math. Prob. Eng. 2014 (2014) 1–7.
[11] C.T. Pan, Y.C. Chen, P.H. Lin, C.C. Hsieh, F.T. Hsu, P.H. Lin, et al., Lens of controllable optical field with thin film metallic glasses for UV-LEDs, Opt. Express 22 (Jun) (2014) 14411–14424.